Research Square

Preprints are preliminary reports that have not undergone peer review.
They should not be considered conclusive, used to inform clinical practice,
or referenced by the media as validated information.

Deep Learning-Based Image Analysis of Dried Blood Spots for Hemoglobin Classification in Cattle: A Preliminary Evaluation

Seher Akbar

seherkhalid4@gmail.com

Islamia University: The Islamia University of Bahawalpur Pakistan https://orcid.org/0009-0001-6716-9164

Ayesha Nazir

Islamia University: The Islamia University of Bahawalpur Pakistan

Umer Farooq

Islamia University: The Islamia University of Bahawalpur Pakistan

Asjad Amin

Islamia University: The Islamia University of Bahawalpur Pakistan

Musadiq Idris

Islamia University: The Islamia University of Bahawalpur Pakistan

Khalid Mansoor

Islamia University: The Islamia University of Bahawalpur Pakistan

Mushtaq Hussain Lashari

Islamia University: The Islamia University of Bahawalpur Pakistan

Maryam Chaudhary

Islamia University: The Islamia University of Bahawalpur Pakistan

Research Article

Keywords: Deep learning models. Image analysis. Dried blood spots. Hemoglobin. Cattle

Posted Date: November 5th, 2026

DOI: https://doi.org/10.21203/rs.3.rs-11270002/v1

License: This work is licensed under a Creative Commons Attribution 4.0 International License.
Read Full License

Abstract

Hemoglobin (Hb, measured in g/dL) is one of the most reliable predictors of anemia in livestock. However, traditional laboratory methods for Hb estimation are invasive, costly, and require specialized equipment, limiting their use in resource-limited settings. Dried blood spot (DBS) sampling offers a practical alternative for quantifying Hb as a less invasive and cost-effective method. This study trained deep learning (DL) models using smartphone-captured images of DBS samples to classify Hb levels in Cholistani cattle. The DBS images were used to create a labeled dataset (Low, Normal, High Hb levels) using reference values from the reference-standard hematology analyzer. The dataset was then randomly divided into training (70%), validation (20%), and testing (10%) subsets to train DL models, including a customized convolutional neural network (CNN), EfficientNetV2-B0, and MobileNetV2. The CNN model achieved the best performance with an overall classification accuracy of 87%, followed by EfficientNetV2-B0 at 76%, and MobileNetV2 at 73%. The preliminary findings suggested that a custom CNN can extract meaningful Hb-related information from DBS images and has the potential to establish an inexpensive, image-based anemia screening tool for resource-limited settings.

Introduction

Hemoglobin (Hb) concentration is a core indicator of anemia and general health in cattle (Jung et al. 2024). Automated hematology analyzers remain the reference method for measuring it. However, their cost, maintenance, and reagent requirements, along with their reliance on trained personnel, limit their use in resource-limited and remote settings (Neogi et al. 2018; Srivastava et al. 2014). Transporting fresh blood to distant laboratories adds a further constraint (Chaudhary et al. 2024). Dried blood spot (DBS) sampling offers a practical alternative, as spotted samples can be stored and transported with minimal handling (McDade et al. 2007). Dried blood spot has been applied to hematological assessment (Capiau et al. 2018), hormone assay (Gruenstein, 2024; Melo et al. 2022; Stauch et al. 2025), metabolic profiling (Allaway et al. 2022; Bardhi et al. 2025; Haijes et al. 2019), and toxicological monitoring (Raju et al. 2016; Velghe et al. 2018) in human and veterinary contexts. As Hb absorbs visible light strongly, the color and spread of a DBS vary with the blood's hematocrit and Hb content (Denniff and Spooner, 2010; Meng et al. 2023). Image analysis of DBS has therefore been used to estimate hematocrit from gray values and spot area (Barroso et al. 2023), and reflectance measurements have been used to predict hematocrit and correct assay bias (Capiau et al. 2018). A web-based tool has also been developed to evaluate spot quality (Veenhof et al. 2019). In small ruminants, image classification combined with machine learning (ML) has been used to detect anemia from PCV (Siddique et al. 2024), and ML has been applied to dried-droplet images to discriminate physiological states in humans (Hamadeh et al. 2020). These approaches, however, rely on manually extracted features such as color values, spot area, and optical density (Barroso et al. 2023; Capiau et al. 2018; Siddique et al. 2024), and target hematocrit rather than Hb directly. Machine learning methods such as support vector machines (SVMs) and decision trees classify images using features (Avanzo et al. 2024); however, deep learning (DL), particularly convolutional neural networks (CNNs), learns discriminative features directly from images (LeCun et al. 2015) and has been applied widely in human and veterinary imaging. Landmark architectures include

residual networks (He et al. 2016) and U-Net (Ronneberger et al. 2015). Smartphone photographs have already been used to estimate Hb from color in fingernail beds (Mannino et al. 2018), which shows that Hb-related information can be recovered from consumer-camera images. The main limitation of DL is its need for large labelled datasets. Transfer learning from ImageNet-pretrained networks such as MobileNetV2 (Sandler et al. 2018) and EfficientNetV2 (Tan and Le, 2021) is widely used to address this, although its benefits for medical images are debated (Raghu et al. 2019). In Veterinary medicine, CNNs have been used to segment medial retropharyngeal lymph nodes on canine CT (Schmid et al. 2022) and to detect pulmonary abnormalities on feline thoracic radiographs (Dumortier et al. 2022).

Veterinary DL work has focused mainly on radiographs, MRI, and ultrasound. To our knowledge, DL has not been applied to DBS images for Hb classification in livestock. We therefore evaluated a custom CNN and two ImageNet-pre-trained models, *viz.* EfficientNetV2-B0 and MobileNetV2, for classifying Hb levels from smartphone-captured images of DBS in Cholistani cattle.

Materials and methods

Animals and study location

Blood samples were collected from apparently healthy indigenous Cholistani cattle (n = 28) reared at the university livestock farm under an intensive farming system. The study included 21 females and 7 males ranging from approximately 1–10 years of age. The hematological analysis and data acquisition were carried out in the postgraduate laboratory, Department of Physiology at Islamia University of Bahawalpur (IUB). All animals on the farm received the same feeding and management routine and had free access to water. Veterinarians conducted regular health assessments of all animals through clinical examinations and blood tests. Systematic and periodic anthelmintic treatments were consistently provided. Farm staff and farm records were consulted to verify each animal's health status, and a complete blood count (CBC) confirmed it. Before collecting blood samples from each animal, their temperature, pulse rate, and respiratory rate were measured.

Blood collection and analysis

Venous blood (3 mL) was collected from the jugular vein of the Cholistani cattle using disposable syringes (10mL). The collected blood was transferred into purple-topped EDTA-filled vacutainers, stored in an icebox, and transported to the laboratory (approximately 3Km, 20 min) for analysis. Blood collection was performed by the same personnel at the same time to ensure standardization of the process. Blood samples were first analyzed for Hb reference values using a pre-validated automated veterinary hematology analyzer (Rayto-RT 7600, China) after homogeneous mixing in a roller mixer (MixR-40, Daihan Scientific, Korea). Then a 20 µL aliquot was spotted onto filter paper (Whatman 42, Sigma-Aldrich, Germany) using a calibrated single-channel micropipette (Dragon Lab, China). This filter paper has been previously validated for Hb estimation by the DBS technique (Chaudhary et al. 2024).

Blood spots were then labelled and allowed to air-dry on a nonabsorbent surface, protected from dust and direct lighting at room temperature for 24 h before imaging.

Image acquisition

A smartphone (Realme C51; Realme, China) with a 50MP primary lens was used to photograph the DBS samples. The smartphone was mounted horizontally, face down, at a distance of approximately 9 cm from the filter paper to maintain focus and framing and ensure consistent lighting across all DBS samples. A plain, non-reflective background was used to minimize any interference from surrounding objects and color variation across different samples. Images were captured natively at the original image resolution (3072 x 4080 pixels) and saved as JPEGs.

Dataset preparation and augmentation

The raw DBS images were transferred to a laptop and processed through a standardized pipeline consisting of cropping and quality checks. Each image was assessed for uniform lighting, clarity, and focus. Images with smudges, incomplete blood spots, or visible artifacts were eliminated to ensure dataset quality.

To remove background noise and center the region of interest (ROI), each image was manually cropped to 300 × 300 pixels using Microsoft Paint 3D, giving N = 735. This patch-based approach provided a localized view of the DBS, enabling the DL models to capture robust color and texture variations correlated with Hb levels. The DBS images were labeled as Low (6–7 g/dL, anemia), Normal (8–12 g/dL, reference range), and High (14–16 g/dL, polycythemia/elevated) Hb levels based on the established veterinary reference ranges (Constable et al. 2017). Data augmentation was applied to the training dataset to improve model generalization and balance the data across classes. To preserve Hb-related visual characteristics, augmentation techniques such as image flipping and rotation were used (Fig. 1).

Custom convolutional neural network architecture

A compact CNN was designed to classify DBS images into three Hb levels. The architecture consists of three convolutional blocks, each consisting of a 3 x 3 convolution (padding, ReLU activation) with 32, 64, and 128 filters, respectively, followed by a 2x2 max-pooling. The extracted feature maps were flattened and passed to a dense layer of 128 units (ReLU) with 50% dropout and a three-unit softmax output layer (Fig. 2).

Transfer learning models

We used two ImageNet-pretrained architectures, EfficientNetV2-B0 and MobileNetV2 (width multiplier 1.0), which are also commonly applied to medical image classification (Al Moteri et al. 2024; Indraswari

et al. 2022; Riaz et al. 2023), to compare classification accuracy with the custom CNN. The original classification layers were removed, and the input size was 300 x 300 x 3. A new classification head was added, with global average pooling, 50% dropout, a dense layer (256 units, ReLU), batch normalization, 30% dropout, and a three-unit softmax layer. Both networks were trained identically in two phases.

Training protocol for deep learning models

All models were trained with the Adam optimizer and categorical cross-entropy loss, using a batch size of 32. Models were implemented in Python version 3 and TensorFlow 2.x using CPU (Google Compute Engine backend) hardware acceleration.

Custom CNN

The custom CNN model was trained in a single phase for 30 epochs at a learning rate of 0.001, without early stopping or learning-rate scheduling. Pixel values were rescaled by 1/255, and weights from the epoch with the lowest validation loss were used for testing.

Transfer learning models

We trained MobileNetV2 and EfficientNetV2-B0 using a two-phase approach. In phase 1, the pretrained base was frozen, and only the new head was trained for 15 epochs (learning rate of 1e-3). In phase 2, 30% of the base layers were unfrozen for fine-tuning; the model was recompiled, and training continued for up to 15 epochs (30 overall) at a learning rate of 1e-4. To avoid overfitting, early stopping (patience = 10 epochs, restoring the best weights) and learning-rate reduction on plateaus (factor 0.5, patience 5, minimum learning rate = 1e-7) were applied. The only preprocessing performed was rescaling pixel values by 1/255.

Performance evaluation

Confusion Matrix Heatmap(s) were drawn to visualize the classification performance of the custom CNN, EfficientNetV2-B0, and MobileNetV2 models. For each class, precision = TP / (TP + FP), recall = TP / (TP + FN), and F1-score = 2 × (precision × recall) / (precision + recall), where TP, FP, and FN denote true positives, false positives, and false negatives. Overall accuracy was the number of correctly classified images divided by the total number of test images. We report precision, recall, and F1-score as unweighted means across the three classes, along with per-class values.

Results

Evaluation metrics

The classification performance for the three DL models, custom CNN, EfficientNetV2-B0, and MobileNetV2, was assessed using evaluation metrics (Table 1). Among the three models, the custom CNN model achieved the best performance with a classification accuracy of 87%, followed by EfficientNetV2-B0 at 76%, and MobileNetV2 at 73%.

Table 1
Classification evaluation metrics for custom convolutional neural network, EfficientNetV2-B0, and MobileNetV2

Deep learning architectures	F1-Score	Precision	Recall	Accuracy
Custom convolutional neural network	0.850	0.889	0.848	87%
EfficientNetV2-B0	0.740	0.756	0.743	76%
MobileNetV2	0.696	0.764	0.701	73%

Confusion matrix analysis

Custom CNN architecture

The confusion matrix of the CNN revealed classification across three classes (Low, Normal, High Hb levels). The Normal class exhibited the highest accuracy, with 46 correctly classified images out of 47 (97.9%), demonstrating the model's robustness in classifying Normal Hb levels. The High class followed with 44 correct classifications out of 48 (91.7%), while the Low class achieved 22 correct predictions out of 34 (64.7%) (Fig. 3).

EfficientNetV2-B0

The EfficientNetV2-B0 exhibited confusion across all classes, with severely misclassified samples, and achieved an overall accuracy of 76%. The Normal class displayed 41 correctly classified samples out of 47 (87.2%), with 2 misclassified as Low and 4 as High. The High class followed, with 40 correctly classified out of 48 (83.3%), with 6 misclassified as Low and 2 as Normal. The Low class attained only 18 correctly classified out of 34 (52.9%), with 12 misclassified as Normal and 2 as High. The model showed restrained classification performance across three classes (Fig. 4).

MobileNetV2

MobileNetV2 achieved an overall accuracy of 73.6% with 47 Normal images correctly classified (100%), indicating zero false negatives for the Normal class. The model showed a strong bias toward predicting Normal; however, 22 Low samples and 6 High samples were misclassified as Normal, making Normal the class with the highest number of false positives. The low class was the weakest, with only 12 correctly classified out of 34 (35.3%), and the remaining 22 were misclassified as Normal. The high class achieved 36 correctly classified out of 48 (75.0%), with 6 misclassified as Low and 6 as Normal (Fig. 5).

Discussion

This study demonstrated that a custom CNN can classify Hb levels from the DBS images. The CNN achieved a reliable accuracy of 87% with balanced precision of 0.889, recall of 0.848, and an F1-score of 0.850 across three classes, outperforming both ImageNet pre-trained models evaluated under identical conditions. The findings indicate that the custom CNN directly learned from subtle Hb-related features, color intensity, and spatial distribution patterns across DBS images, which were more discriminative than general-purpose features transferred from natural-image pretraining. While, to our knowledge, DBS-based Hb classification with DL in livestock has not been previously attempted, a closely related work on non-invasive, image-based anemia and Hb classification via palpebral conjunctiva delivers results identical to our study.

Smartphone-based, image-driven anemia classification using ML and DL has been reported with accuracies broadly in the 72–96% range, depending on dataset size, imaging conditions, and model choice. A study by Suner et al. (2021) achieved 72% accuracy in predicting anemia from smartphone conjunctival images using an ML model, with 73% sensitivity and 83% specificity. Moreover, Kedar et al. (2025) reported that a customized CNN for conjunctiva-based anemia detection reached 96% accuracy and outperformed both MobileNet and ResNet50.

In the present study, recall for the Low Hb class was comparatively limited across all three models (CNN 64.7%, EfficientNetV2-B0 52.9%, MobileNet 35.3%). A similar pattern has been reported in closely related human conjunctiva-based work: Kato et al. (2024) found that a CNN trained on a limited, imbalanced dataset for smartphone conjunctival images achieved high specificity but markedly reduced sensitivity for the anemic class. These findings suggest that difficulty in detecting the minority, clinically relevant class is a recurring challenge for image-based Hb/anemia classification generally, though confirming this is a general phenomenon would require a dedicated comparative or systematic analysis.

The comparatively lower performance of EfficientNetV2-B0 and MobileNetV2 relative to the custom CNN may reflect a genuine domain gap between natural-image pretraining and the relatively homogeneous, texture-driven appearance of DBS images, consistent with reports that transfer-learning benefits are constrained as the target domain diverges from ImageNet (Zhou et al. 2017). It should be noted, however, that EfficientNetV2-B0 and MobileNetV2 require different input preprocessing, and this comparison assumes that scaling was applied correctly and consistently for each architecture.

These findings should be regarded as preliminary. The dataset was limited to 28 animals from a single farm and imaged under controlled conditions (fixed lighting, standardized distance, and a specific mobile phone model), which may limit generalizability across other breeds, environments, or camera hardware; manual patch cropping may have introduced additional variability. Future work should prioritize a larger, multi-site dataset, ideally with an animal-level validation strategy, to confirm the present findings and improve detection of Low-Hb cases specifically. If confirmed, integrating the custom CNN into a smartphone application with real-time image-quality feedback would be a reasonable next step toward field-deployable anemia screening in cattle.

Conclusion

The study provides preliminary evidence that the proposed architecture can reliably extract and learn color and textural features of DBS images that are relevant to Hb concentration. A custom CNN classified Hb status from smartphone-captured images of DBS in cattle with 87% accuracy, outperforming two ImageNet-pre-trained architectures under identical conditions. Across three models, classification accuracy was least reliable for anemic (Low-Hb) animals, the group most relevant to clinical screening. Given the limited sample size of 28 animals from a single farm, these results are preliminary and require confirmation in a larger, multi-site cohort to support the development of a smartphone-based, low-cost Hb classification in cattle in resource-limited settings.

Declarations

Competing interests

The authors have no relevant financial or non-financial interests to disclose.

Ethics approval

Ethical approval was obtained from the Departmental Research Ethics Committee, Department of Physiology, The Islamia University of Bahawalpur, Pakistan (Ref. No. PHYSIO-87/2025–134, dated 13th of August 2025). Utmost ethical standards were maintained for animal handling and management.

Funding

The authors declare that no funds, grants, or other support were received during the preparation of this manuscript.

Author contributions

All authors contributed to the study conception and design. Material preparation, data collection and analysis were performed by Seher Akbar, Ayesha Nazir, Umer Farooq, Asjad Amin, Musadiq Idris, Khalid Mansoor, Mushtaq Hussain Lashari, Maryam Chaudhary. The first draft of the manuscript was written by Seher Akbar and all authors commented on previous versions of the manuscript. All authors read and approved the final manuscript.

Data availability

The datasets generated during the current study are not publicly available but are available from the corresponding author on reasonable request.

References

1. Al Moteri M, Mahesh TR, Thakur A, Vinoth Kumar V, Khan SB, Alojail M (2024) Enhancing accessibility for improved diagnosis with modified EfficientNetV2-S and cyclic learning rate strategy in women with disabilities and breast cancer. Front Med 11:1373244. https://doi.org/10.3389/fmed.2024.1373244
2. Allaway D, Alexander JE, Carvell-Miller LJ, Reynolds RM, Winder CL, Weber RJM, Lloyd GR, Southam AD, Dunn WB (2022) Suitability of dried blood spots for accelerating veterinary biobank collections and identifying metabolomics biomarkers with minimal resources. Front Vet Sci 9:887163. https://doi.org/10.3389/fvets.2022.887163
3. Avanzo M, Stancanello J, Pirrone G, Drigo A, Retico A (2024) The evolution of artificial intelligence in medical imaging: from computer science to machine and deep learning. Cancers 16(21):3702. https://doi.org/10.3390/cancers16213702
4. Bardhi A, Barbarossa A, Joubert A, Gehring R, Lambertini C, Romagnoli N (2025) The suitability of dried blood spot sampling for pharmacokinetic studies in veterinary medicine. Vet Sci 12(5):488. https://doi.org/10.3390/vetsci12050488
5. Barroso MG, Gustafsson L, Barclay V, Linder C (2023) A validated method for the determination of hematocrit in dried blood spots using image analysis. Bioanalysis 15(6):331–341. https://doi.org/10.4155/bio-2023-0018
6. Capiau S, Wilk LS, De Kesel PMM, Aalders MCG, Stove CP (2018) Correction for the hematocrit bias in dried blood spot analysis using a nondestructive, single-wavelength reflectance-based hematocrit prediction method. Anal Chem 90(3):1795–1804. https://doi.org/10.1021/acs.analchem.7b03784
7. Chaudhary M, Farooq U, Idris M, Lashari MH, Qasim S, Afzal MA, Khan MA, Ali A (2024) First report on clinical feasibility of dried blood spot technique for hemoglobin estimation in Cholistani cattle. Adv Life Sci 11(3):663–668. https://doi.org/10.62940/als.v11i3.2993
8. Constable PD, Hinchcliff KW, Done SH, Grünberg W (2017) Veterinary medicine: a textbook of the diseases of cattle, horses, sheep, pigs, and goats, 11th edn. Elsevier, St Louis
9. Denniff P, Spooner N (2010) The effect of hematocrit on assay bias when using DBS samples for the quantitative bioanalysis of drugs. Bioanalysis 2(8):1385–1395. https://doi.org/10.4155/bio.10.103
10. Dumortier L, Guépin F, Delignette-Muller ML, Boulocher C, Grenier T (2022) Deep learning in veterinary medicine, an approach based on CNN to detect pulmonary abnormalities from lateral thoracic radiographs in cats. Sci Rep 12:11418. https://doi.org/10.1038/s41598-022-14993-2
11. Gruenstein Y (2024) Validation of a dried blood spot assay for testosterone measurement using liquid chromatography- tandem mass spectrometry. Anal Sci Adv 5(11–12):e202400035. https://doi.org/10.1002/ansa.202400035

12. Haijes HA, Willemsen M, van der Ham M, Gerrits J, Pras-Raves ML, Prinsen HCMT, Verhoeven-Duif NM, Janssens S, van Hasselt PM (2019) Direct infusion based metabolomics identifies metabolic disease in patients' dried blood spots and plasma. Metabolites 9(1):12. https://doi.org/10.3390/metabo9010012
13. Hamadeh L, Imran S, Bencsik M, Sharpe GR, Johnson MA, Fairhurst DJ (2020) Machine learning analysis for quantitative discrimination of dried blood droplets. Sci Rep 10:3313. https://doi.org/10.1038/s41598-020-59847-x
14. He K, Zhang X, Ren S, Sun J (2016) Deep residual learning for image recognition. In: Proceedings of the IEEE conference on computer vision and pattern recognition. IEEE, pp 770–778
15. Indraswari R, Rokhana R, Herulambang W (2022) Melanoma image classification based on MobileNetV2 network. Procedia Comput Sci 197:198–207. https://doi.org/10.1016/j.procs.2021.12.132
16. Jung Y, Ku JY, Kim Y, Kim W, So H, Piao L, Yoon JS, Park J (2024) Identification of hemolytic anemia in Korean indigenous cattle with a criteria value of reticulocyte count, indirect bilirubin, and L-lactate concentration. Front Vet Sci 11:1375518. https://doi.org/10.3389/fvets.2024.1375518
17. Kato S, Chagi K, Takagi Y, Hidaka M, Inoue S, Sekiguchi M, Adachi N, Sato K, Kawai H, Kato M (2024) Machine/deep learning-assisted hemoglobin level prediction using palpebral conjunctival images taken by a smartphone. Br J Haematol 205:1590–1598. https://doi.org/10.1111/bjh.19621
18. Kedar DS, Pandey G, Koolagudi SG (2025) Non-invasive detection of anemia using deep learning on conjunctival images. In: 2025 International Conference on Artificial Intelligence and Data Engineering (AIDE). IEEE, pp 718–724. https://doi.org/10.1109/AIDE64228.2025.10987403
19. LeCun Y, Bengio Y, Hinton G (2015) Deep learning. Nature 521(7553):436–444. https://doi.org/10.1038/nature14539
20. Mannino RG, Myers DR, Tyburski EA, Caruso C, Boudreaux J, Leong T, Clifford GD, Lam WA (2018) Smartphone app for non-invasive detection of anemia using only patient-sourced photos. Nat Commun 9:4924. https://doi.org/10.1038/s41467-018-07262-2
21. McDade TW, Williams S, Snodgrass JJ (2007) What a drop can do: dried blood spots as a minimally invasive method for integrating biomarkers into population-based research. Demography 44(4):899–925. https://doi.org/10.1353/dem.2007.0038
22. Melo AM, Silva JS, Claudio JM, Amaral RS (2022) Evaluation of the use of dry blood spots for progesterone determination in ewes. Acta Vet Bras 16(4):305–308. https://doi.org/10.21708/avb.2022.16.4.10932
23. Meng Z, Tayyab M, Lin Z, Raji H, Javanmard M (2023) A smartphone-based disposable hemoglobin sensor based on colorimetric analysis. Sensors 23(1):394. https://doi.org/10.3390/s23010394
24. Neogi SB, Negandhi H, Sharma J, Ray S, Saxena R (2018) Diagnostic efficacy of digital hemoglobinometer (TrueHb), HemoCue and non invasive devices for screening patients for anemia in the field settings – a proposal. Indian J Community Health 30(Suppl 1):86–88.

25. Raghu M, Zhang C, Kleinberg J, Bengio S (2019) Transfusion: understanding transfer learning for medical imaging. Adv Neural Inf Process Syst 32.
26. Raju KSR, Taneja I, Rashid M, Sonkar AK, Wahajuddin M, Singh SP (2016) DBS-platform for biomonitoring and toxicokinetics of toxicants: proof of concept using LC-MS/MS analysis of fipronil and its metabolites in blood. Sci Rep 6:22447. https://doi.org/10.1038/srep22447
27. Riaz Z, Khan B, Abdullah S, Khan S, Islam MS (2023) Lung tumor image segmentation from computer tomography images using MobileNetV2 and transfer learning. Bioengineering 10(8):981. https://doi.org/10.3390/bioengineering10080981
28. Ronneberger O, Fischer P, Brox T (2015) U-Net: convolutional networks for biomedical image segmentation. In: Navab N, Hornegger J, Wells WM, Frangi AF (eds) Medical image computing and computer-assisted intervention – MICCAI 2015. Lecture notes in computer science, vol 9351. Springer, Cham, pp 234–241. https://doi.org/10.1007/978-3-319-24574-4_28
29. Sandler M, Howard A, Zhu M, Zhmoginov A, Chen LC (2018) MobileNetV2: inverted residuals and linear bottlenecks. In: Proceedings of the IEEE conference on computer vision and pattern recognition (CVPR). IEEE, pp 4510–4520
30. Schmid D, Scholz VB, Kircher PR, Lautenschlaeger IE (2022) Employing deep convolutional neural networks for segmenting the medial retropharyngeal lymph nodes in CT studies of dogs. Vet Radiol Ultrasound 63(6):763–770. https://doi.org/10.1111/vru.13132
31. Siddique A, Panda SS, Khan S, Dargan ST, Lewis S, Carter I, Van Wyk JA, Mahapatra AK, Morgan ER, Terrill TH (2024) Innovations in animal health: artificial intelligence-enhanced hematocrit analysis for rapid anemia detection in small ruminants. Front Vet Sci 11:1493403. https://doi.org/10.3389/fvets.2024.1493403
32. Srivastava T, Negandhi H, Neogi SB, Sharma J, Saxena R (2014) Methods for hemoglobin estimation: a review of “what works”. J Hematol Transfus 2(3):1028
33. Stauch W, Olausson J, Bendes A, Beck O, Schwenk JM (2025) Multiplex quantification of endocrine proteins in volumetric dried blood spots. Clin Proteomics 22(1):18. https://doi.org/10.1186/s12014-025-09539-3
34. Suner S, Rayner J, Ozturan IU, Hogan G, Meehan CP, Chambers AB, Baird J, Jay GD (2021) Prediction of anemia and estimation of hemoglobin concentration using a smartphone and machine learning techniques. PLoS One 16:e0253495. https://doi.org/10.1371/journal.pone.0253495
35. Tan M, Le QV (2021) EfficientNetV2: smaller models and faster training. In: Proceedings of the 38th international conference on machine learning (PMLR 139), pp 10096–10106
36. Veenhof H, Koster R, Brinkman R, Senturk E, Bakker S, Berger S, Akkerman OW, Touw DJ, Alffenaar JWC (2019) Performance of a web-based application measuring spot quality in dried blood spot sampling. Clin Chem Lab Med 57(12):1846–1853. https://doi.org/10.1515/cclm-2019-0437
37. Velghe S, De Troyer R, Stove C (2018) Dried blood spots in therapeutic drug monitoring and toxicology. Expert Opin Drug Metab Toxicol 14(1):1–3. https://doi.org/10.1080/17425255.2018.1414181

38. Zhou Z, Shin J, Zhang L, Gurudu S, Gotway M, Liang J (2017) Fine-tuning convolutional neural networks for biomedical image analysis: actively and incrementally. In: Proceedings of the IEEE conference on computer vision and pattern recognition. IEEE, Honolulu, pp 4761–4772

Figures

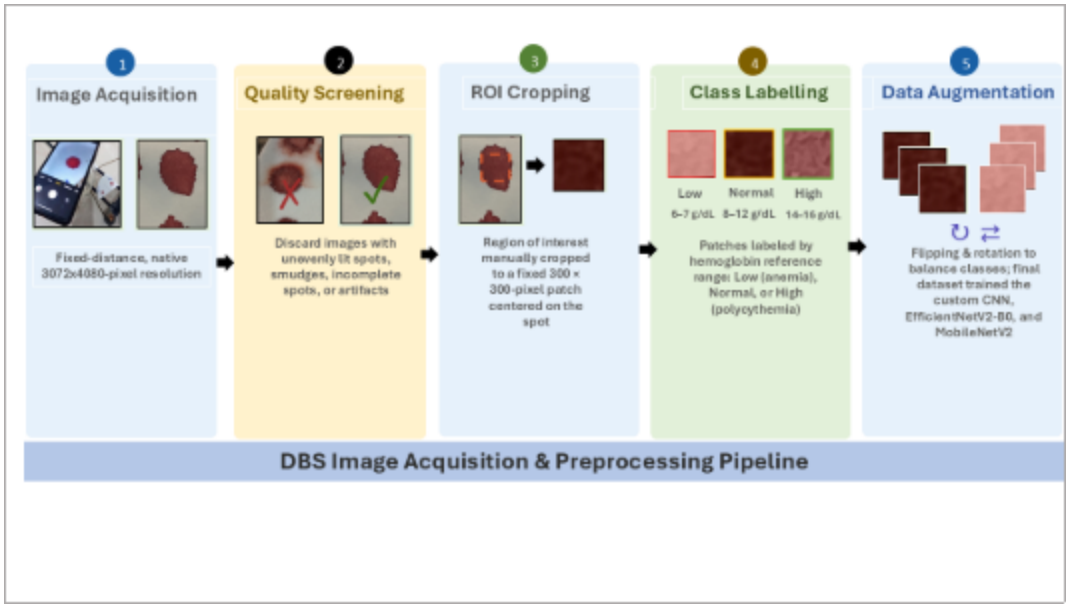


Figure 1

Systematic workflow of the image acquisition and data processing pipeline. (1) Photography of the smartphone imaging environment utilizing a clear support structure to maintain a fixed 8-10 cm distance and visual layout of a representative raw dried blood spot (DBS) image at the native 3072 × 4080-pixel resolution. (2) Quality screening of each DBS image. (3) Demonstration of the Manual Region of Interest (ROI) selection process executed using pixel grid coordinates in Microsoft Paint 3D. (4) Patch labelling according to reference values obtained from the hematology analyzer. (5) Data augmentation to balance class representation in the final dataset used for model training.

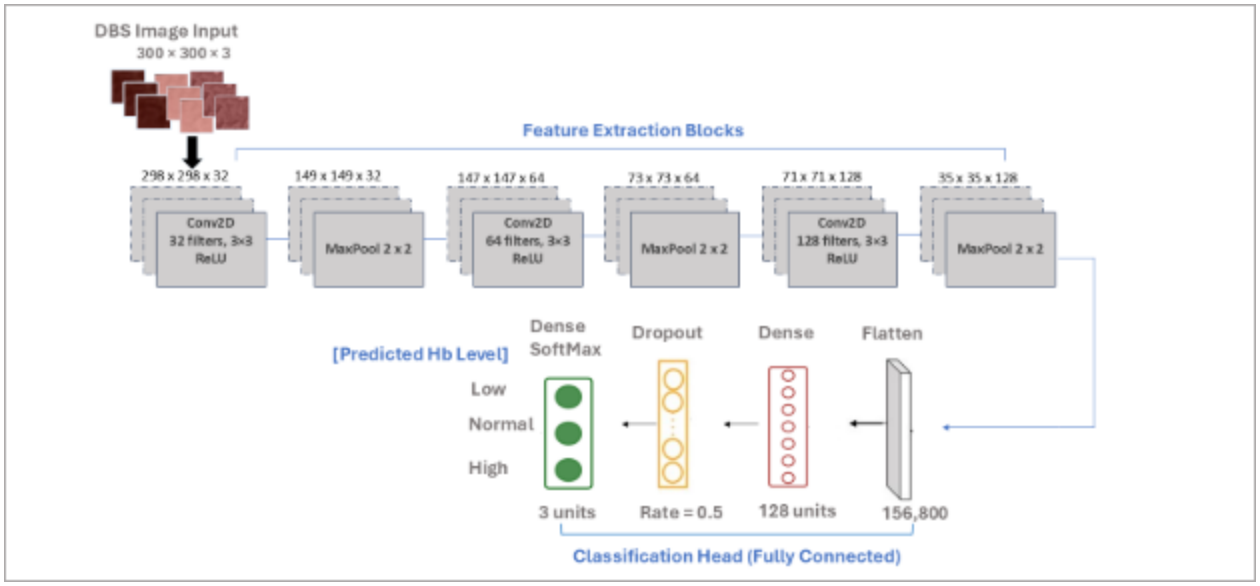


Figure 2

Architecture of the proposed customized convolutional neural network (CNN) for classification of hemoglobin (Hb) levels from dried blood spot (DBS) images. Three Conv2D-MaxPool blocks (32/64/128filters, 3x3, ReLU) extract features from the 300 x 300 x 3 input image, followed by a flattening layer, a dense layer (128 units, ReLU, dropout = 0.5), and a Softmax output classifying Hb levels as Low, Normal, or High.

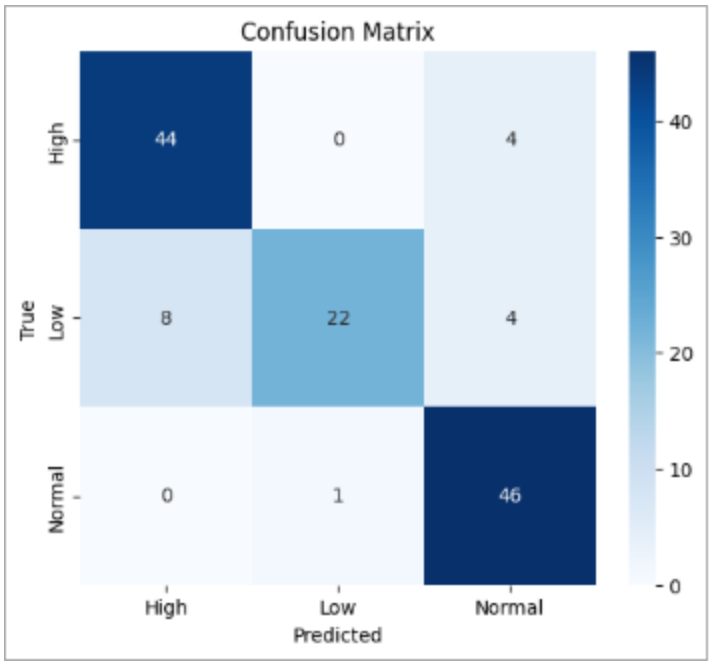


Figure 3

Confusion matrix of a custom convolutional neural network (CNN) for hemoglobin (Hb) classification using dried blood spot (DBS) images. The matrix illustrates the distribution of predictions across 3 Hb classes: Low, Normal, and High.

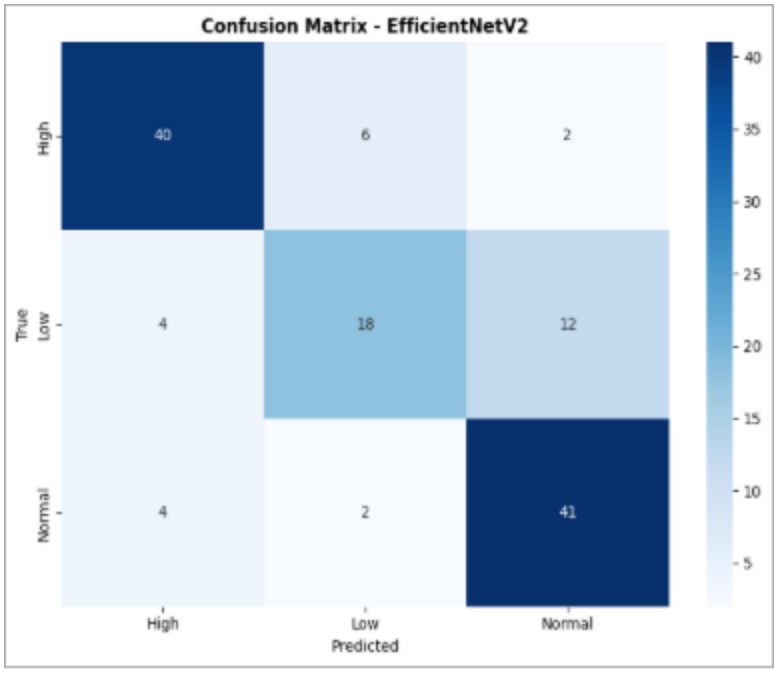


Figure 4

Confusion matrix of EfficientNetV2-B0 for hemoglobin classification using dried blood spot images.

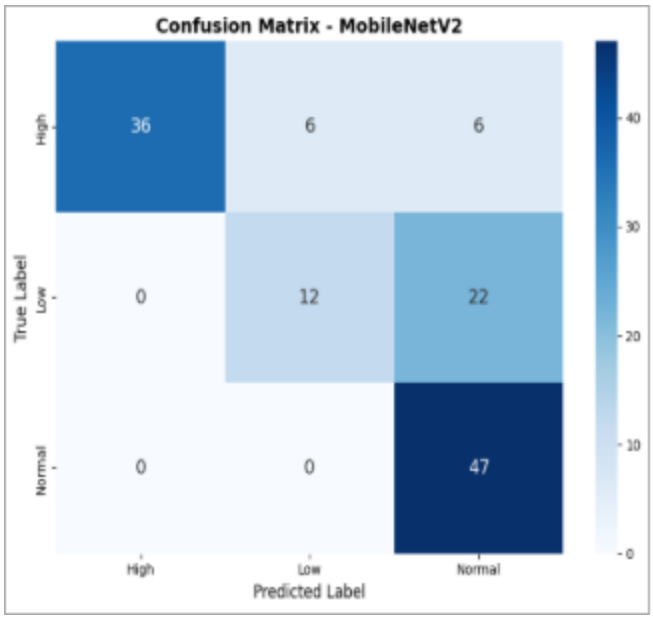


Figure 5

Confusion matrix of MobileNetV2 for hemoglobin classification using dried blood spot images.